LEGIBILITY NOTICE

A major purpose of the Technical Information Center is to provide the broadest dissemination possible of information contained in DOE's Research and Development Reports to business, industry, the academic community, and federal, state and local governments.

Although a small portion of this report is not reproducible, it is being made available to expedite the availability of information on the research discussed herein.

LA-UR -87-2803

Los Alamos National Laboratory is operated by the University of California for the United States Department of Energy under contract W-7405 ENG 36

LA-UR--87-2803

DE87 014768

TITLE NUMERICAL MODELING OF SLOW SHOCKS

AUTHOR(S) D. Winske, X-1

SUBMITTED TO Proceedings of Solar Wind Six, Estes Park, CO, August 25-28, 1987

DISCLAIMER

MASTER

Los Alamos Los Alamos National Laboratory
Los Alamos, New Mexico 87545

Numerical Modeling of Slow Shocks

D. Winske
Los Alamos National Laboratory
Los Alamos, NM 87545

Abstract

This paper reviews previous attempts and the present status of efforts to understand the structure of slow shocks by means of time dependent numerical calculations. Studies carried out using MHD or hybrid-kinetic codes have demonstrated qualitative agreement with theory. A number of unresolved issues related to hybrid simulations of the internal shock structure are discussed in some detail.

1. Introduction

Shock waves are of interest to a large segment of the space and astrophysical community on a wide range of levels. On a universal level shock waves are an efficient mechanism for producing energetic particles, e.g., cosmic rays. On a smaller scale (< solar system), shocks are discontinuities associated with the solar wind (e.g., interplanetary shocks, planetary bow shocks, terminator shock, etc.). On an even shorter scale (many km) shocks are a most interesting plasma physics engine that converts directed particle motion into random energy and plasma waves. However, when one thinks of shock waves, almost always one has in mind fast shocks [upstream flow speed exceeds the fast (magnetosonic) speed], e.g., the contents of the recent AGU monographs on shocks [Stone and Tsurutani, 1985; Tsurutani and Stone, 1985]. Slow shocks [upstream flow speed exceeds the slow mode speed, but is less than the intermediate (Alfven) speed] also exist, but occur much less frequently. A few slow shocks have been identified in the solar wind [Chao and Olbert, 1970; Burlaga and Chao, 1971; Richter *et al.*, 1985; Richter, 1988] and in the magnetotail [Feldman *et al.*, 1984a, 1984b, 1985, 1987; Smith *et al.*, 1984; Feldman, 1988], which have provided all that is known about their internal structure. The lack of a large data base of observations has led to an equally small theoretical effort. Except for Coroniti's [1971] detailed investigation of the internal magnetic structure of slow shocks, there have been few other theoretical [Kantrowitz and Petschek, 1966; Neubauer, 1976; Hada and Kennel, 1985; Edmiston and Kennel, 1986; Schwartz *et al.*, 1987; Wolfson, 1987; Kennel, 1988] or numerical [Hayashi and Sato, 1978, Sato *et al.*, 1978; Sato, 1979; Swift, 1983, Winske *et al.*, 1985a] studies. On a more macroscopic scale, in addition to occurring in the solar wind and magnetotail, slow shocks have been postulated to occur in coronal holes [Whang, 1982, 1986], to be associated with coronal mass ejecta [Hundhausen *et al.*, 1987] and to be part of fast-slow shock systems [Whang, 1987]. However, more understanding of how slow shocks work is needed before their importance relative to fast shocks in accelerating particles and as a potential source of cosmic rays can be assessed.

The purpose of this paper is to review previous work of slow shock structure obtained from time dependent numerical calculations. As the number of such investigations and the amount of definitive conclusions obtained from them is rather small, this is not a complicated task. Combined with other unpublished work, a number of unresolved issues related to modeling slow mode shocks can be enumerated. These are discussed in some detail and are presented here as promising areas for future research.

2. Review of Previous Work

In this section previous work involving simulations of slow shocks is reviewed. Two types of numerical models have been employed: MHD and hybrid-kinetic. The MHD calculations [Hayashi and Sato, 1978; Sato *et al.*, 1978; Sato, 1979] use a standard 2-D MHD resistive model to study magnetic reconnection. The slow shocks form at the interface between the external and boundary layer regions, consistent with the Petschek model [1964]. The hybrid-kinetic studies [Swift, 1983; Winske *et al*, 1985a] are one-dimensional and include ion kinetic effects using particle in cell methods and treat the electrons as a massless fluid. [See Winske (1985) for a review of the numerical methods involved.] In contrast to the more global MHD calculations, the hybrid simulations focus on the intrinsic structure of the shock. Here we briefly review what is known theoretically about slow mode shocks and then describe the results of the various simulations and relate them to theory.

A. Theory

Slow shocks have two interesting and important features. First, the overall transition from upstream to downstream is characterized by an increasing density jump (and corresponding decrease of the normal floww speed) accompanied by a decreasing magnetic field, as can be inferred from the Rankine-Hugoniot relations [Edmiston and Kennel, 1986]. As a result, the magnetic field is bent toward the shock normal in the downstream region. A macroscopic consequence is that the bow shock which forms in front of an obstacle in the flow bends toward the upstream, rather than the downstream [e.g., see Figure 1, Wolfson (1987)]. On the other hand, the plasma flow in the downstream is larger and is bent away from the normal direction. Because the plasma pressure and magnetic pressure change in opposite directions across the shock, it is not always easy to identify slow shock crossings from other types of MHD discontinuities. Richter *et al.* [1985] have provided a practical test to distinguish between these types of configurations.

The second significant feature of slow shocks is the magnetic wavetrain which trails behind the leading edge of the shock [Coroniti, 1971]. The shock layer that separates the upstream and downstream states is made up of a series of magnetic field rotations of decreasing amplitude. Using MHD equations with finite ion Larmor radius corrections, Coroniti has shown that the wavelength of the rotation is related to the ion inertial length at low beta or the ion gyroradius at high beta, while the damping length depends on the magnitude of the dissipation. For weak resistivitites the damping can be very small and

many rotations of the magnetic field are expected [e.g., see Figure 2, Coroniti (1971)]. Observationally, only the slow shock in the near earth magnetotail [Feldman *et al.*, 1987] exhibits some sort of trailing wavetrain. The lack of a wavetrain at other slow shocks may be due to instrumental limitations or physics issues to be discussed later.

B. MHD Simulations

The principal purpose of the MHD simulations was to study driven magnetic reconnection with various types of boundary conditions and values for the resistivity. The simulations produce an X-point with four slow shocks radiating from it, as proposed by Petschek [1964]. Figure 1, adapted from Hayashi and Sato [1978] shows the 3-D current structure (left) and the cross-sectional structure of the slow mode shocks (right). In the left panel, the plasma in injected from the right and left sides and flows out along the top and bottom of the figure. The characteristic slow shock form, mass density (ρ) and pressure (p) rising across the shock (at x=0.5) while the magnetic field (B_x shown) is reduced, is clearly visible. A detailed analysis of these shocks [Sato, 1979] demonstrates that the shocks are slow mode and that the Rankine-Hugoniot relations are obeyed. In such calculations neither the ion inertial length or the ion gyroradius are resolved, so no wavetrain is generated. Such calculation, however, show that strong flows (jets) occur along the plasma sheet boundary layer downstream of the shocks. Thus, the overall structure of the slow shock with decreasing magnetic field bent toward the normal and increasing plasma flow away from the normal is reproduced.

C. Hybrid Simulations

In the hybrid-kinetic simulations a different approach is followed. These calculations use particle ions and fluid electrons to look at the intrinsic shock structure in one spatial dimension [Swift, 1983; Winske *et al.*, 1985a]. Because the ions are treated kinetically, ion inertia and gyroradius effects are naturally included, so that the trailing wavetrain can be studied. Such types of calculations allow examination of the fine details of slow shocks on ion-like scales; similar methods have been most successful in understanding fast shocks Leroy *et al.*, 1982; Quest, 1987]. There are, however, a number of unresolved issues associated with hybrid code simualtions of slow shocks. These are discussed in the next section, where the results of previous simulations are also described. Here we merely point out that the past work [Swift, 1983] has led to three major conclusions. First, as with the shocks produced in the MHD treatments, the shock profiles generated with the hybrid simulations are consistent with the Rankine-Hugoniot solutions: namely, oppositely directed density and magnetic field jumps and accelerated plasma flows. Second, the hybrid simulations demonstrate the existence of the trailing wavetrain structure predicted by Coroniti [1971], showing that broad shock transitions are indeed possible. Third, the calculations show large fluxes of ions streaming upstream from the shock, as were seen for example at the slow shock in the near earth magnetotail [Feldman *et al.*, 1987] and in the plasma sheet boundary layer [Tsurutani *et al.*, 1985]. These results emphasize that the non-MHD nature of slow shocks requires a kinetic ion treatment to model them accurately.

3. Issues

While hybrid simulations have been shown to offer an improved technique for studying slow mode shocks, there are a number of unsolved problems associated with using such methods. These are discussed at some length in this section.

A. Shock Formation

One of three methods can be used to initialize simulations of slow shocks. First, one can start with uniform upstream and downstream states related by Rankine-Hugoniot conditions, as used by Swift [1983] and by Leroy *et al.* [1982] for fast shocks, and let the system then evolve in time. Figure 2 shows how the shock is formed. Displayed are v_x-x and v_x-x phase space for the ions and profiles of the density (n) and magnetic field component (B_z). The left panel shows the initial state: upstream state to the left, downstream to the right. The parameters in this case are: shock normal angle $\theta_{Bn} = 60°$, Alfven Mach number $M_A = 0.5$, upstream ion beta $\beta_i = 0.01$, and upstream electron beta $\beta_e = 0.1$. These conditions correspond to a switch off shock, so that $B_z = 0$ downstream. Note, consistent with the Rankine-Hugoniot relations, that the downstream ion z velocity is larger than the upstream normal (x) velocity and that the downstream ions are much hotter than the upstream ions. In this calculation the electrons are assumed to be adiabatic ($T_e \sim n^{\gamma-1}$). The middle panels show the same results at $\Omega_i t = 25$. Plasma is continuously injected at the left boundary to maintain a uniform upstream state. The density profile shows that a steep shock front is still present, but some hot ions have leaked ahead of the shock from downstream A magnetic wavetrain has started to form. At later time ($\Omega_i t = 50$), the wavetrain has extended further downstream and the shock front is more diffuse as ions continue to leak upstream [Swift, 1983]. Later, we will show the same shock at a further point in time and discuss more of the results.

A second method to form shocks is to let the incident plasma stream reflect off the right wall of the system. The ions then couple via some instability to produce a hot plasma near the wall and the shock propagates back toward the upstream. This method has the advantage that no presupposed downstream state is assumed. Such a technique has been used successfully by Quest [1987] for generating parallel shocks. The same method was used by Winske *et al.* [1985a] for producing slow shocks, as shown in Figure 3. While this scheme gives a well defined shock front, it has two major drawbacks: first, the wavetrain forms right at the wall; second, one must run the calculation to very long times in order to get the shock away from the boundary.

A third method is to form the slow shock from a steepened slow wave. The difficulty here is that numerical dispersion limits the amount of steepening. Hada and Kennel [1985] have examined the steepening rate of slow waves, but did not produce shocks by this method. Hada *et al.* [1987] and Omidi and Winske [1987] observed steepened fast waves in hybrid simulations of foreshock phenomena, but again the pulses did not form true shock-like structures.

A major difficulty with all of these methods is that the shock formation time ($\Omega_i t > 50$, Ω_i= upstream ion gyrofrequency) is very long, which translates into significant computational costs ($\sim$ 1 Cray hour for 1-D shocks). More complete calculations in two dimensions would be prohibitively expensive. Clearly, more efficient methods to initialize slow shock simulations in which remnants of the initial state or the boundary conditions do not play a significant role are needed. Calculations with more realistic initial conditions may help to explain why so few slow shocks are observed in the solar wind.

B. Shock Structure

Figure 4 shows profiles of the slow shock of Figure 2 at much later times ($\Omega_i t = 200$): v_x-x and v_z-x ion phase space, and profiles of the density (n), magnetic field magnitude (B) and B_z. One notices that the wavetrain now extends farther downstream; the waves decrease in amplitude and wavelength with distance from the front of the shock. In v_x-x space it is seen that the hot downstream ions continue to leak through the shock. These backstreaming ions are also seen in v_z-x space, but in this panel the predominant feature are the large excursions of the ions in the downstream region. By comparing with the B_z profile, it is evident that the ions follow the magnetic field through the shock. The ion density increases gradually through the shock layer from upstream to the downstream state; the layer width continues to expand in time as the wavetrain grows [Coroniti, 1971]. The magnetic field magnitude (B) rises slightly above its upstream value at the start of the wavetrain, then decays to its downstream value.

We have also carried out a number of simulations for a variety of upstream conditions [Stover and Winske, unpublished]. Results of some of these runs showing the magnetic wavetrain are displayed in Figure 5. In each case profiles of B_y versus x are shown at the same time ($\Omega_i t = 200$) for conditions similar to those in Figure 2, except as noted. The only difference with the case given in the previous figures is that here the initial downstream ions are colder and the electrons are ohmically heated, as discussed later. The top three panels of Figure 5 compare cases with different upstream ion beta (β_i=0.001, 0.01, 0.1). Generally, the wavelength and damping coefficient increase with β_i. The next three panels compare switch off shocks at various θ_{Bn} [θ_{Bn} = 75° (M_A = .26), 45° (.71), 30° (.87)]: the wavelength and damping decrement decrease with θ_{Bn}. The last panel displays the wavetrain for a shock away from the switch off limit: θ_{Bn} = 55°, M_A = 0.5. Compared to the switch off case at M_A = 0.5, the amplitude is smaller, the wavelength is slightly shorter and the damping is stronger away from switch off.

A preliminary analysis of the wavelengths calculated in the simulations and the theoretical results of Coroniti [1971] (his low beta linearized equations, 4.1-4.2) has been carried out [Stover and Winske, unpublished]. Overall, there is rough agreement, and again it is an area for more study: both to include more of the physics in the numerical solutions of the wavetrain equations as well as to carry out better analysis of the simulations. It should also be noted that the damping in the simulation decreases with time toward the fluid limit Winske *et al.* [1985a]. The larger damping in the higher ion beta case may suggest kinetic as well as resistive damping may be important [Swift, 1983]. Alternatively,

the higher ion beta may merely give rise to more rapid phase mixing and thus destruction of the coherent wavetrain sooner [Quest, private communication].

C. Electron Model

Another unresolved issue is the proper electron model to use. The underlying philosophy of the hybrid method is that the electrons are relatively unimportant and ion effects dominant. On the other hand, Hada *et al.* [unpublished] have shown that the wave properties of the slow mode change with beta (i.e., double adiabatic or kinetic electron models give slow waves with phase speeds greater than the intermediate speed at high beta) and argue for the need for a CGL equation of state in the simulations. For the calculations in the last subsection the electrons were either adiabatic or ohmically heated with a resistivity $\bar{\eta} = \eta 4\pi/\omega_i = 2 \times 10^{-6}$. Other electron models (e.g., T_e=constant) are possible as well. Figure 6 compares the wavetrains of slow shocks at the same time for the same upstream conditions (same as Figure 2) when the electrons are: (a) adiabatically heated (with $\gamma = 5/3$), (b) ohmically heated, and (c) isothermal. The results show some difference in the wavetrain structure. The ohmically heated case has the longest wavetrain, the adiabatic case has the strongest damped wavetrain, while the isothermal case has the least wavetrain damping just behind the shock front. The wavelengths are slightly different in each case as well.

D. Potentials

A fourth interesting, but not well studied feature of slow shocks is the role of the electrostatic potential. Recent work [Schwartz *et al.*, 1987, and references therein] has shown that the electrostatic potential is frame dependent. In the de Hoffman Teller frame, which corresponds to moving along the upstream or downstream magnetic field, there is no motional electric field and the change in the electron energy is directly related to ϕ in this frame (ϕ^{HT}). For fast shocks $\phi^{HT} \ll \phi^{NI}$, where ϕ^{NI} is the potential in the frame where the plasma is normally incident on the shock (e.g., the simulation frame), implying that the electron gain at fast shocks is much less than that lost by the ions. On the other hand, for a slow shock $\phi^{HT} > \phi^{NI}$ [Schwartz *et al.*, 1987], indicating that the electron gain is greater than the ion loss. Figure 7 shows profiles of ϕ^{NI} and ϕ^{HT} for the same shock shown in Figure 4. Although ϕ^{NI} is large, $\sim$ the ion incident energy ($E_o = m_i V_o^2/2$) at the shock, the ions are not reflected electrostatically, because they follow the magnetic field rotations through the shock. The profile of ϕ^{NI} has a very similar shape to that of B_y (cf. top panel of Figure 6). In this case the electron temperature change across the shock is about the upstream temperature and $\phi^{HT}/E_o \sim 1$. For comparison, the bottom panel of Figure 7 shows ϕ^{HT} for the case with resistively heated electrons (corresponding to the top panel in Figure 6). In this case the electron temperature jump, and thus ϕ^{HT}, is somewhat larger.

E. Ion Dynamics

The behavior of ions at slow shocks is also an area where little is known, but hybrid

simulations can be most useful. As mentioned earlier, the incoming ions follow the magnetic wavetrain through the shock. This behavior can be understood from the following argument.

The force on the ions in the y direction is given by

$$F_y = e(E_y + V_z B_x - V_x B_z)$$

In the upstream region, $F_y = 0$ and since $V_z = 0$, this implies the motional electric field, $E_y = V_{x1} B_{z1}$. In the downstream region of the switch off shock, $B_z = 0$ and since E_y is constant across the shock, $V_{x2} = -E_y/B_x = -V_{x1} B_{z1}/B_x$, which in general gives accelerated flows ($V_2 > V_1$) in the downstream region. However, if one imagines that the shock switches off rapidly, then just at the switch off point, V_z is still zero from the upstream, but B_z is now zero, so that $F_y > 0$. The ions will thus accelerate in the y direction. Once they have received this kick in the y direction, they gyrate about the downstream field (B_x). The transverse ion velocity and the magnetic field vary together ($V_y \sim B_y$, $V_z \sim B_z$), as can be inferred from Eqns. 2.7-2.8 of Coroniti [1971], leading to the formation of the wavetrain.

In addition, a number of ions ($< 10\%$) return upstream [Swift, 1983; Winske *et al.*, 1985a]. While particle orbits of incoming ions [Stover and Winske, unpublished] show that some of the ions are turned around deep in the shock layer, most of the backstreaming ions in Figure 4 come from the downstream population. To demonstrate this more clearly, we replot the v_x-x phase space and B_z profile from Figure 4 on the top half of Figure 8. The middle panels correspond to another simulation with the same parameters as Figure 4, but with ohmically heated electrons and correspondingly colder downstream ions. Several curious features appear. First, there are less backstreaming ions at the front of the wavetrain, suggesting the colder ions cannot catch up to the shock easily [Edmiston and Kennel, 1986]. Second, as noted in Figure 6, the magnetic wavetrain is much longer and cleaner, which suggests there is less damping because of the colder ions. Third, the shock tends to drift upstream somewhat. Finally, upstream of the start of the wavetrain there is an expanding gradual bulge on B_z that propagates upstream and slows the incident ions well upstream of the shock transition. It again points out the need to be careful in initializing these kinds of simulations. More observations of ions escaping from the front of slow shocks will be a major help in selecting proper downstream states as well the electron equation of state to use in the calculations.

F. Alpha Particles

Usually, alpha particles comprise a small, but not insignificant fraction of the solar wind population. Richter *et al.* [1985] have shown for their interplanetary slow shock that the alpha particle contribution to the Rankine-Hugoniot relations is important to obtain the proper shock conditions. An interesting question is what happens to such ions when they encounter a slow shock. Simulations of fast shocks show that heavy ions tend to be unaffected by the electric field at the shock front. Instead, they propagate into the downstream region, where they gyrate in the stronger magnetic field and perhaps return

to the shock front [Winske *et al.*, 1985b; Omidi *et al.*, 1986]. The bottom panel of Figure 8 shows v_x-x phase space for alpha particles at late time ($\Omega_i t = 300$) in a simulation identical to that in the middle panels. Like the protons, the alpha particles follow the magnetic field through the shock. Far downstream the alphas phase mix and are left strongly heated, but it is not clear whether any of them can eventually leak back upstream. Although the alpha particles comprise 5% of the incident population in this case, the structure of the shock and the wavetrain are not changed significantly.

G. Dissipation

The important feature of most of the slow shocks that have observed in the solar wind and the magnetotail is the absence of the trailing magnetic wavetrain. While this may be due to a lack of temporal resolution in the measurements (interplanetary shocks traveling past the spacecraft too fast), or in the case of the magnetotail, to not enough room in the boundary layer to fit in a wavetrain, an alternative explanation is that the wavetrain is damped by a large (anomalous) resistivity. Because the density and magnetic field gradients are antiparallel, the mostly likely candidate to produce such a resistivity is the lower hybrid drift instability [e.g., Lemons and Gary, 1978]. However, there is little evidence from plasma wave [Scarf *et al.*, 1984; Coroniti *et al.*, unpublished] or electron measurements [Schwartz *et al.*, 1987] in the magnetotail that strong wave particle scattering is occurring. Plasma heating by high frequency, ion acoustic waves is also a possibility, but like at the subcritical fast shock, the ion acoustic turbulence level is probably too low to be important for heating [Winske *et al.*, 1987], although the presence of ion acoustic like waves may suggest the existence of backstreaming ions [Greenstadt and Mellott, 1987]. So far, however, a detailed study of possible microinstabilities and their effect at the leading edge of the current layer of a slow shock has not been carried out.

H. 2-D Effects

Another explanation for the absence of a wavetrain may be that it is destroyed by 2-D effects, not included in the present 1-D simulations. For example, the Alfven ion cyclotron instability, which is excited by a temperature anisotropy in the ions ($T_{i\perp} > T_{i\parallel}$), operates at fast shocks and isotropizes the ions in the downstream region [Thomas and Brecht, 1986]. As noted previously, the absence of a good method to initialize a slow shock simulation implies that the calculations must be run to a very long time in a large system, which precludes a 2-D calculation at the present time. One could conceivably use the results of a 1-D calculation, assuming spatial homogeneity in the second dimension, to initialize the 2-D simulation with a wavetrain already in place. Of course, it is best to understand the 1-D structure as well as possible before extensive studies of 2-D are undertaken.

I. Summary

This rather lengthy list of problems does not constitute a complete set, but is instead

merely a starting point. Some of the questions are rather straightforward and only require some diligent effort. Other are more difficult and need much more thinking through. It is a fair guess to predict that some of these issues will be resolved, but many other will remain by the time of Solar Wind Seven.

4. Conclusions

Time dependent numerical simulations of slow shocks have been reviewed. The MHD calculations show that slow shocks are an important element in magnetic reconnection, but the simulations cannot resolve the trailing wavetrain structure. Such wavetrains are clearly seen in the hybrid-kinetic calculations that include ion inertia and gyroradius scales, but as yet quantitative comparisons with theory have not been carried out. A number of other issues related to particle dynamics and the overall field structure in the hybrid simulations are still unresolved and remain challenging questions to be investigated in the future. Finally, it must be emphasized that successful numerical modeling requires detailed comparison with observations. In order to achieve the level of understanding of slow shocks that presently exists for fast shocks, more complete observations of more slow shocks in the solar wind are needed.

Acknowledgements

This work was performed under the auspices of the US Dept. of Energy and was supported in part by the Defense Nuclear Agency.

References

Burlaga, L. F., and J. K. Chao, Reverse and forward slow shocks in the solar wind, *J. Geophys. Res.*, *76*, 7516, 1971.

Chao, J. K., and S. Olbert, Observation of slow shocks in interplanetary space, *J. Geophys. Res.*, *75*, 6394, 1970.

Coroniti, F. V., Laminar wavetrain structure of collisionless magnetic slow shocks, *Nucl. Fusion*, *11*, 261, 1971.

Edmiston, J. P., and C. F. Kennel, A parametric study of slow shock Rankine-Hugoniot solutions and critical Mach numbers, *J. Geophys. Res.*, *91*, 1361, 1986.

Feldman, W. C., Planetary magnetosphere observations of slow shocks, in *Solar Wind Six*, 1988.

Feldman, W. C., D. N. Baker, S. J. Bame, J. Birn, J. T. Gosling, E. W. Hones, and S. J. Schwartz. Slow mode shocks: a semipermanent feature of the distant geomagnetic tail, *J. Geophys. Res., 90*, 233, 1985.

Feldman, W. C., D. N. Baker, S. J. Bame, J. Birn, E. W. Hones, S. J. Schwartz, and R. L. Tokar, Power dissipation at slow mode shocks in the distant geomagetic tail, *Geophys. Res. Lett., 11*, 1058, 1984a.

Feldman, W. C., S. J. Schwartz, S. J. Bame, D. N. Baker, J. Birn, J. T. Gosling, E. W. Hones, D. J. McComas, J. A. Slavin, E. J. Smith, and R. D. Zwickl, Evidence for slow mode shocks in the deep geomagnetic tail, *Geophys. Res. Lett., 11*, 599, 1984b.

Feldman, W. C., R. L. Tokar, J. Birn, E. W. Hones, S. J. Bame, and C. T. Russell, Structure of a slow mode shock observed in the plasma sheet boundary layer, *J. Geophys. Res., 92*, 83, 1987.

Greenstadt, E. W., and M. M. Mellott, Plasma wave evidence for reflected ions in front of subcritical shocks: ISEE 1 and 2 observations, *J. Geophys. Res., 92*, 4730, 1987.

Hada, T., and C. F. Kennel, Nonlinear evolution of slow waves in the solar wind, *J. Geophys. Res., 90*, 531, 1985.

Hada, T., C. F. Kennel, and T. Terasawa, Excitation of compressional waves and the formation of shocklets in the earth's foreshock, *J. Geophys. Res., 92*, 4423, 1987.

Hayashi, T., and T. Sato, Magnetic reconnection: acceleration, heating, and shock formation, *J. Geophys. Res., 83*, 217, 1978.

Hundhausen, A. J., T. E. Holzer, and B. C. Low, Do slow shocks precede some coronal mass ejections?, *J. Geophys. Res., 92*, in press, 1987.

Kantrowitz, A., and H. E. Petschek, MHD characteristics and shock waves, in *Plasma Physics in Theory and Application*, edited by W. B. Kunkel, p. 143, McGraw-Hill, New York, 1966.

Kennel, C. F., Tutorial on basic physics of slow shocks in astrophysical context, in *Solar Wind Six*, 1988.

Lemons, D. S., and S. P. Gary, Current driven instabilities in a laminar perpendicular shock, *J. Geophys. Res., 83*, 1625, 1978.

Leroy, M. M., D. Winske, C. C. Goodrich, C. S. Wu, and K. Papadopoulos, The structure of perpendicular bow shocks, *J. Geophys. Res., 87*, 5081, 1982.

Neubauer, F. M., Nonlinear interaction of discontinuities in the solar wind and the origin of slow shocks, *J. Geophys. Res., 81*, 2248, 1976.

Omidi, N., and D. Winske, A kinetic study of solar wind mass loading and cometary bow shocks, *J. Geophys. Res., 92*, in press, 1987.

Omidi, N., D. Winske, and C. S. Wu, The effect of heavy ions on the formation and structure of cometary bow shocks, *Icarus, 66*, 165, 1986.

Petschek, H. E., Magnetic field annihilation, in *AAS-NASA Symposium on the Physics of Solar Flares*, edited by W. N. Hess, *NASA Spec. Publ. SP-50*, p. 425, 1964.

Quest, K., Theory and simulation of collisionless parallel shocks, *J. Geophys. Res.*, submitted, 1987.

Richter, A. K., Observations of interplanetary slow shocks, in *Solar Wind Six*, 1988.

Richter, A. K., H. Rosenbauer, F. M. Neubauer, and N. G. Ptitsyna, Solar wind observations associated with a slow forward shock wave at 0.31 AU, *J. Geophys. Res., 90*, 7581, 1985.

Sato, T., Strong plasma acceleration by slow shocks resulting from magnetic reconnection, *J. Geophys. Res., 84*, 7177, 1979.

Sato, T., T. Hayashi, T. Tamao and A. Hasegawa, Confinement and jetting of plasmas by magnetic reconnection, *Phys. Rev. Lett., 41*, 1548, 1978.

Scarf, F. L., F. V. Coroniti, C. F. Kennel, E. J. Smith, J. A. Slavin, B. T. Tsurutani, S. J. Bame, and W. C. Feldman, Plasma wave spectra near slow mode shocks in the distant magnetotail, *Geophys. Res. Lett., 11*, 1050, 1984.

Schwartz, S. J., M. F. Thomsen, W. C. Feldman, and F. T. Douglas, Electron dynamics and potential jump across slow mode shocks, *J. Geophys. Res., 92*, 3165, 1987.

Smith, E. J., J. A. Slavin, B. T. Tsurutani, W. C. Feldman, and S. J. Bame, Slow mode shocks in the earth's magnetotail: ISEE-3, *Geophys. Res. Lett., 11*, 1054, 1984.

Stone, R. G., and B. T. Tsurutani, *Collisionless Shocks in the Heliosphere: A Tutorial Review*, *Geophys. Mongr. Ser. No. 34*, AGU, Washington D. C., 1985.

Swift, D. W., On the structure of the magnetic slow switch off shock, *J. Geophys. Res., 88*, 5685, 1983.

Thomas, V. A., and S. H. Brecht, Two dimensional simulation of high Mach number plasma interactions, *Phys. Fluids, 29*, 2444, 1986.

Tsurutani, B. T., and R. G. Stone, *Collisionless Shocks in the Heliosphere: Reviews of Current Research*, *Geophys. Monogr. Ser. No. 35*, AGU, Washington D. C., 1985.

Tsurutani, B. T., I. G. Richardson, R. M. Thorne, W. Butler, E. J. Smith, S. W. H.

Cowley, S. P Gary, S. I. Akasofu, and R. D. Zwickl, Observations of the right hand resonant ion beam instability in the distant plasma sheet boundary layer, *J. Geophys. Res.*, *90*, 12159, 1985.

Whang, Y. C., Slow shocks around the sun, *Geophys. Res. Lett.*, *9*, 1081, 1982.

Whang, Y. C., Solar wind flow upstream of the coronal slow shock, *Astrophys. J.*, *307*, 838, 1986.

Whang, Y. C., Slow shocks and their transition to fast shocks in the inner solar wind, *J. Geophys. Res.*, *92*, 4349, 1987.

Winske, D., Hybrid simulations codes with application to shocks and upstream waves, *Space Sci. Rev.*, *42*, 53, 1985.

Winske, D., J. Giacalone, M. F. Thomsen, and M. M. Mellott, A comparative study of plasma heating by ion acoustic and modified two stream instabilities at subcritical quasiperpendicular shocks, *J. Geophys. Res.*, *92*, 4411, 1987.

Winske, D., E. K. Stover, and S. P. Gary, The structure and evolution of slow mode shocks, *Geophys. Res. Lett.*, *12*, 295, 1985a.

Winske, D., C. S. Wu, Y. Y. Li, Z. Z. Mou, and S. Y. Guo, Coupling of newborn ions to the solar wind by electromagnetic instabilities and their interaction with the bow shock, *J. Geophys. Res.*, *90*, 2713, 1985b.

Wolfson, R., The configuration of slow mode shocks, *J. Geophys. Res.*, *92*, in press, 1987.

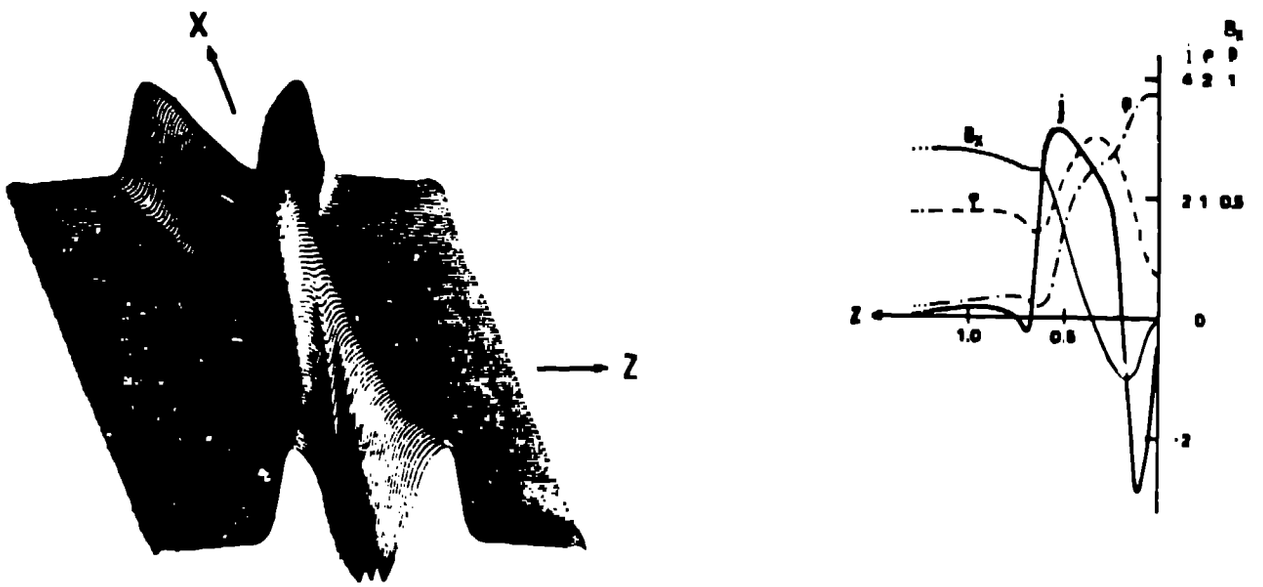

Figure 1. Results of MHD simulations showing slow shock current structure (left panel) in reconnection geometry and profiles of mass density (ρ), pressure (p), magnetic field component (B_z), and current (j) through the shock [from Hayashi and Sato, 1978].

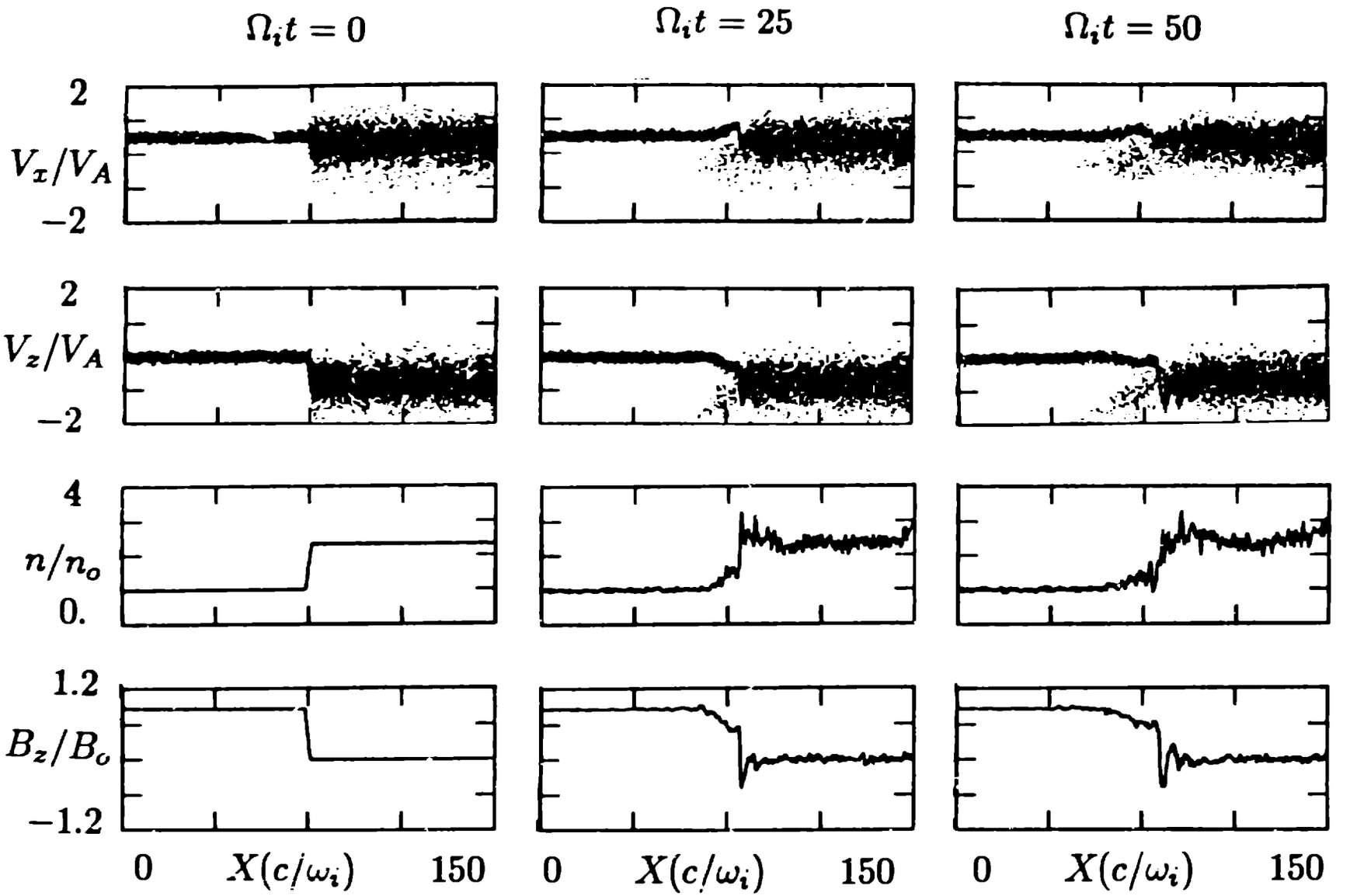

Figure 2. Results of hybrid simulations showing shock formation from initial uniform states related by Rankine-Hugoniot conditions: profiles of v_x-x and v_z-x ion phase space, ion density (n), and magnetic field component (B_z) at various times.

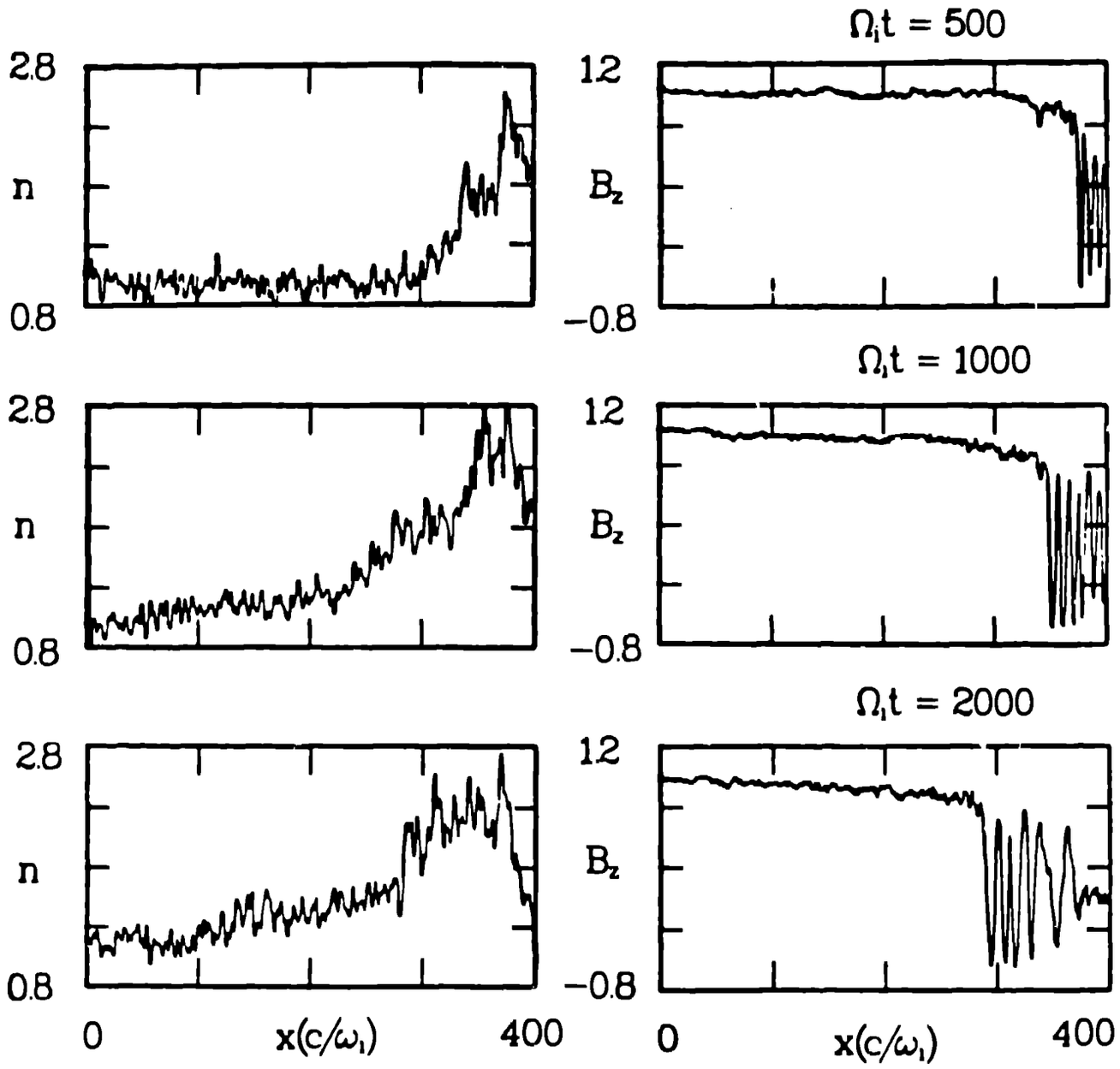

Figure 3. Results of hybrid simulations showing slow shock formation from the interaction of a plasma stream with a reflecting wall: profiles of density and B_z at various times [from Winske *et al.*, 1985].

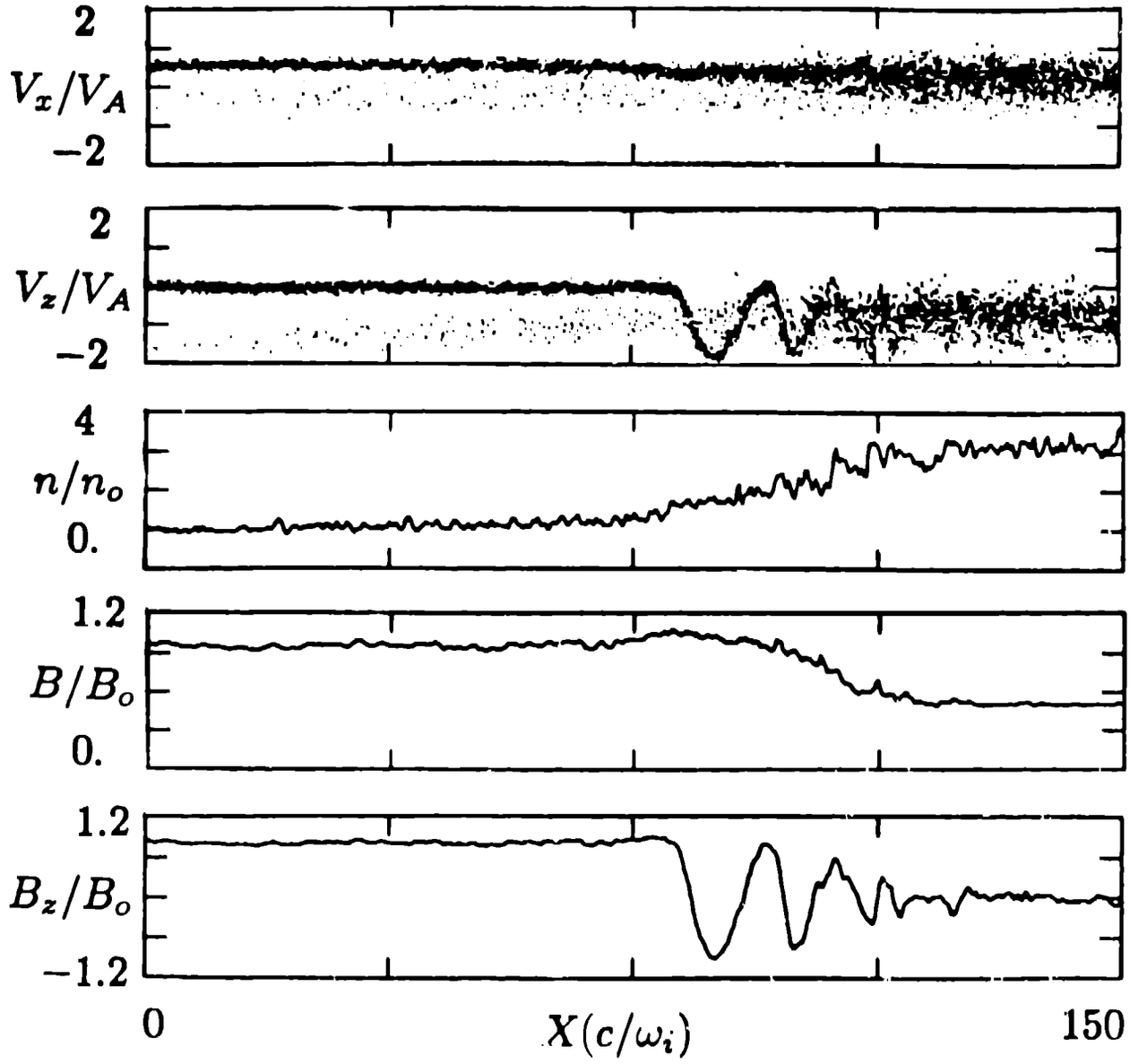

Figure 4. Results of slow shock simulation of Figure 2 at later time ($\Omega_i t = 200$) showing v_x-x, v_z-x phase space and profiles of n, B, and B_z. Parameters in this and subsequent figures unless otherwise noted: $\theta_{Bn} = 60°$, $M_A = 0.5$, $\beta_i = 0.01$, $\beta_e = 0.1$.

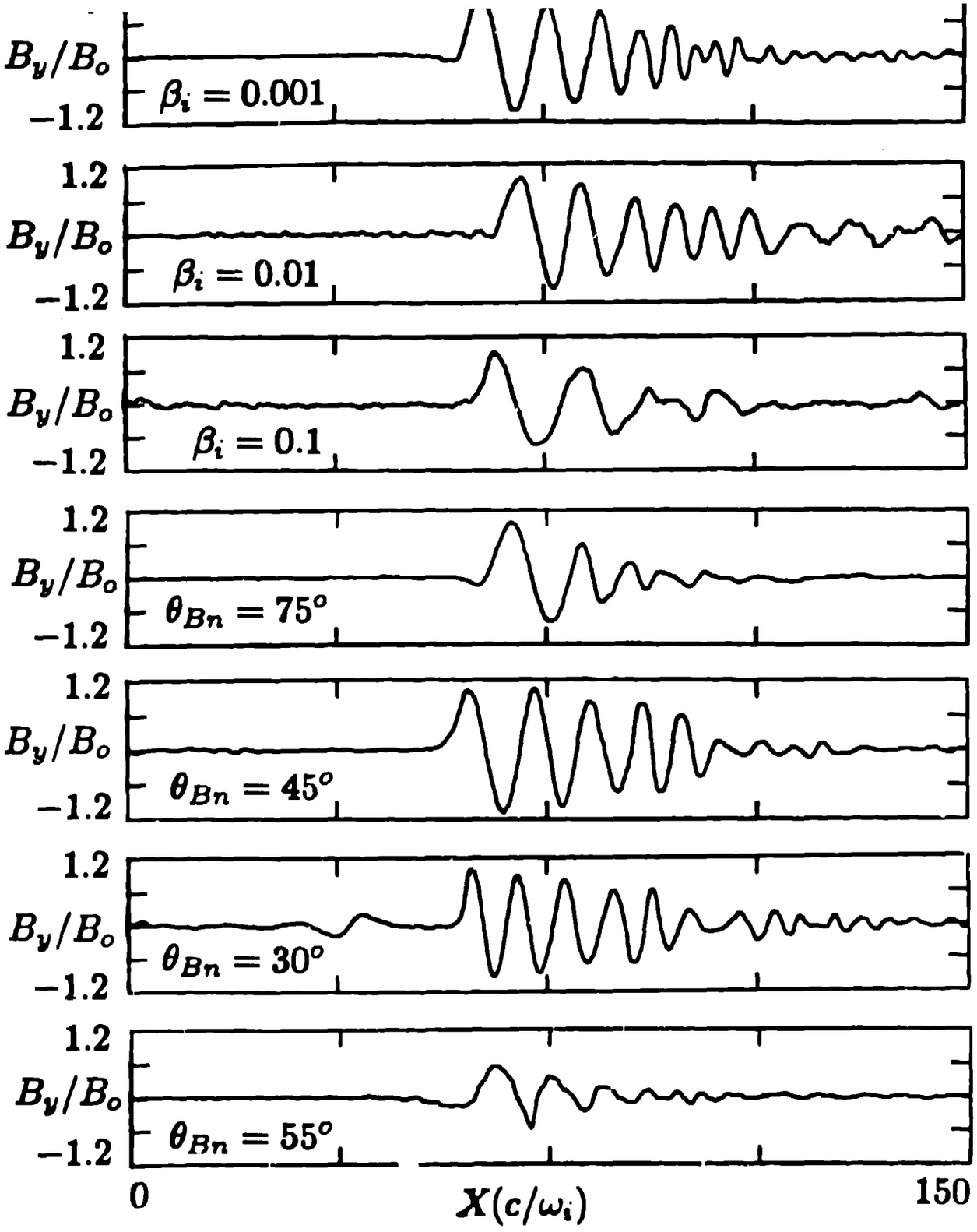

Figure 5. Results of various hybrid simulations showing wavetrain structure in B_y: (a) $\beta_i = 0.001$, (b) $\beta_i = 0.01$, (c) $\beta_i = 0.1$, (d) $\theta_{Bn} = 75^o$ ($M_A = 0.26$), (e) $\theta_{Bn} = 45^o(0.71)$, (f) $\theta_{Bn} = 30^o(0.87)$, (g) $\theta_{Bn} = 55^o(0.5)$.

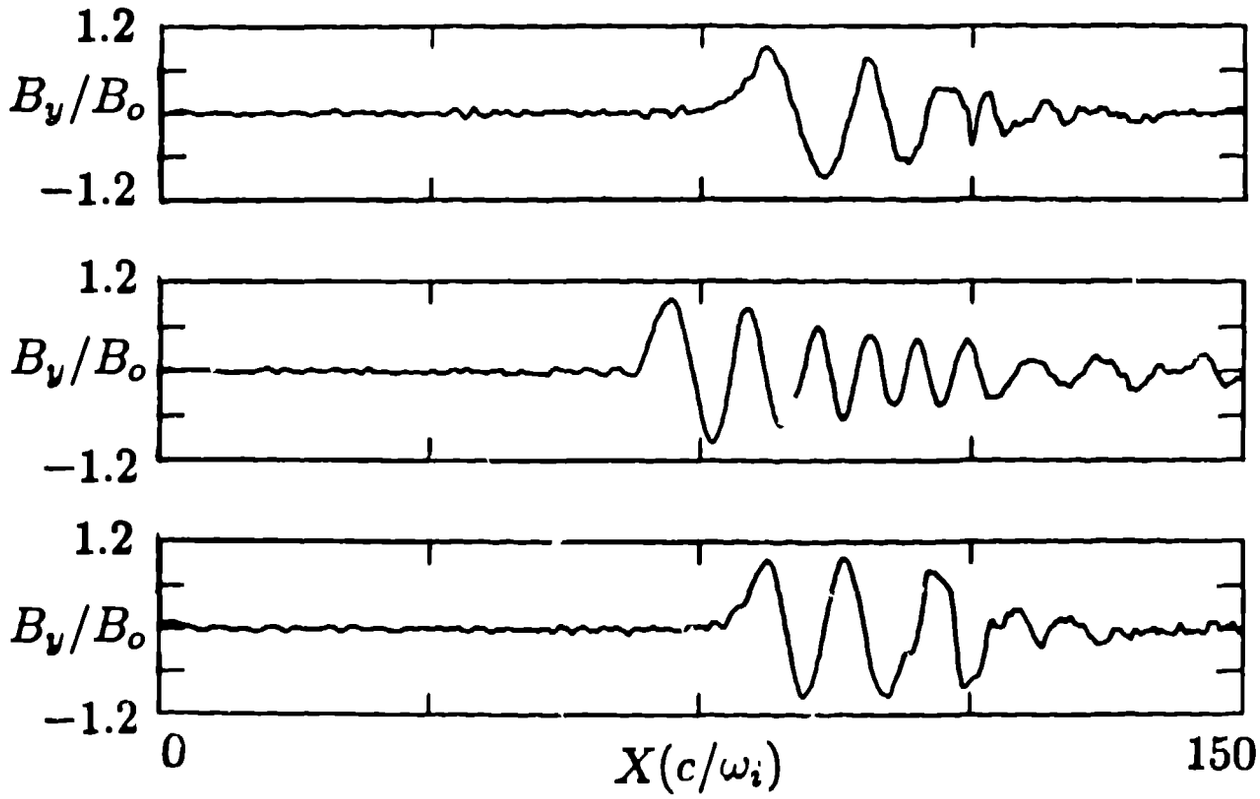

Figure 6. Results of various hybrid simulations showing wavetrain structure in B_y for various electron models: (a) adiabatically heated, (b) ohmically heated, and (c) isothermal.

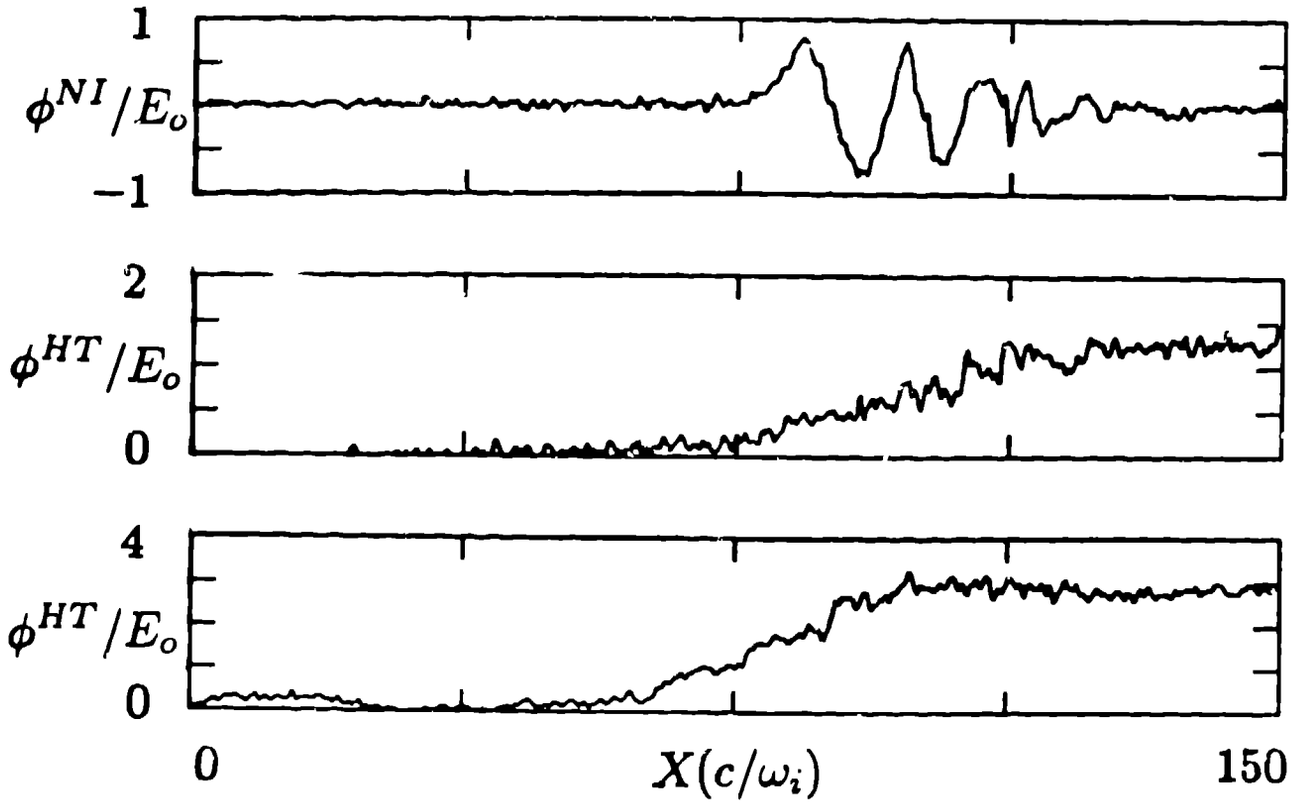

Figure 7. Profiles of electrostatic potentials for same case as Figure 4: (a) ϕ^{NI}, (b) ϕ^{HT}, (c) ϕ^{HT} for similar parameters but ohmically heated electrons.

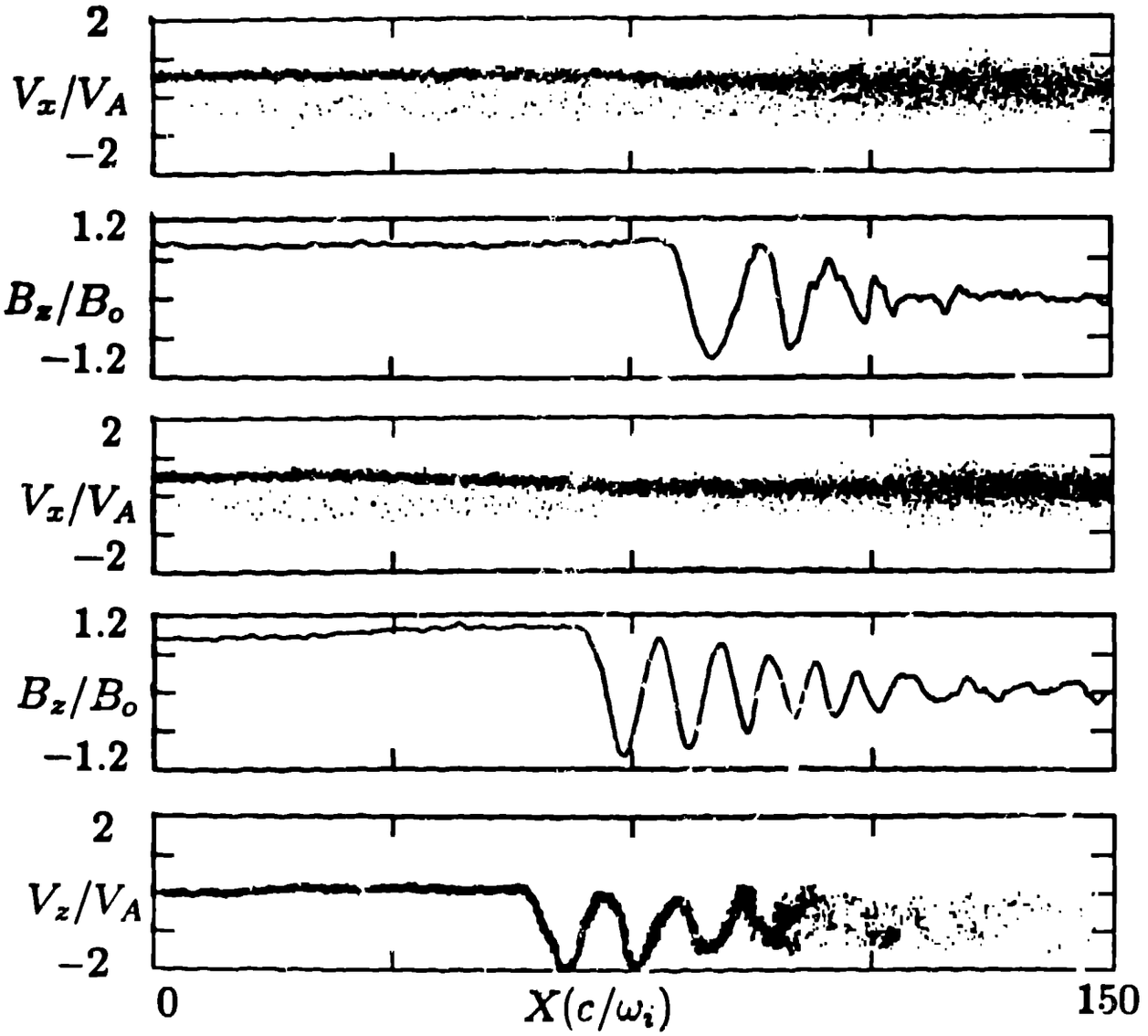

Figure 8. [Top panels]: v_x-x and B_z from Figure 4; [middle panels]: v_x-x and B_z for similar run with ohmically heated electrons; [bottom panel] v_x-x phase space for alpha particles for run similar to the middle panels except that the alpha population is 5% of the upstream density and $\Omega_i t = 300$.